Research Article

For reprint orders, please contact: reprints@futuremedicine.com

Nanomedicine

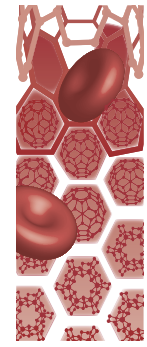

Optimizing the preparation and stability of decorated antiretroviral drug nanocrystals

Tian Zhou[1,2], Zhiyi Lin[1,2], Pavan Puligujja[1], Diana Palandri[1], James Hilaire[1], Mariluz Araínga[1], Nathan Smith[1], Nagsen Gautam[2], JoEllyn McMillan[1], Yazen Alnouti[1], Xinming Liu[1], Benson Edagwa*[,1] & Howard E Gendelman**[,1,2]

[1]Department of Pharmacology & Experimental Neuroscience, University of Nebraska Medical Center, Omaha, NE 68198, USA

[2]Department of Pharmaceutical Sciences, University of Nebraska Medical Center, Omaha, NE 68198, USA

*Author for correspondence: benson.edagwa@unmc.edu

**Author for correspondence: hegendel@unmc.edu

Aim: While the therapeutic potential for current long-acting (LA) antiretroviral therapy (ART) is undeniable, ligand-decorated nanoformulated LA-ART could optimize drug delivery to viral reservoirs. The development of decorated ART hinges, however, on formulation processes and manufacture efficiencies. To this end, we compared manufacture and purification techniques for ligand-decorated antiretroviral drug nanocrystals. **Materials & methods:** Ligand-decorated nanoparticle manufacturing was tested using folic acid (FA) nanoformulated cabotegravir. **Results:** Direct manufacturing of FA-cabotegravir resulted in stable particles with high drug loading and monocyte–macrophage targeting. A one step 'direct' scheme proved superior over differential centrifugation or tangential flow filtration facilitating particle stability and preparation simplicity and efficiency. **Conclusion:** Direct manufacturing of FA nanoparticles provides a path toward large-scale clinical grade manufacturing of cell-targeted LA-ART.

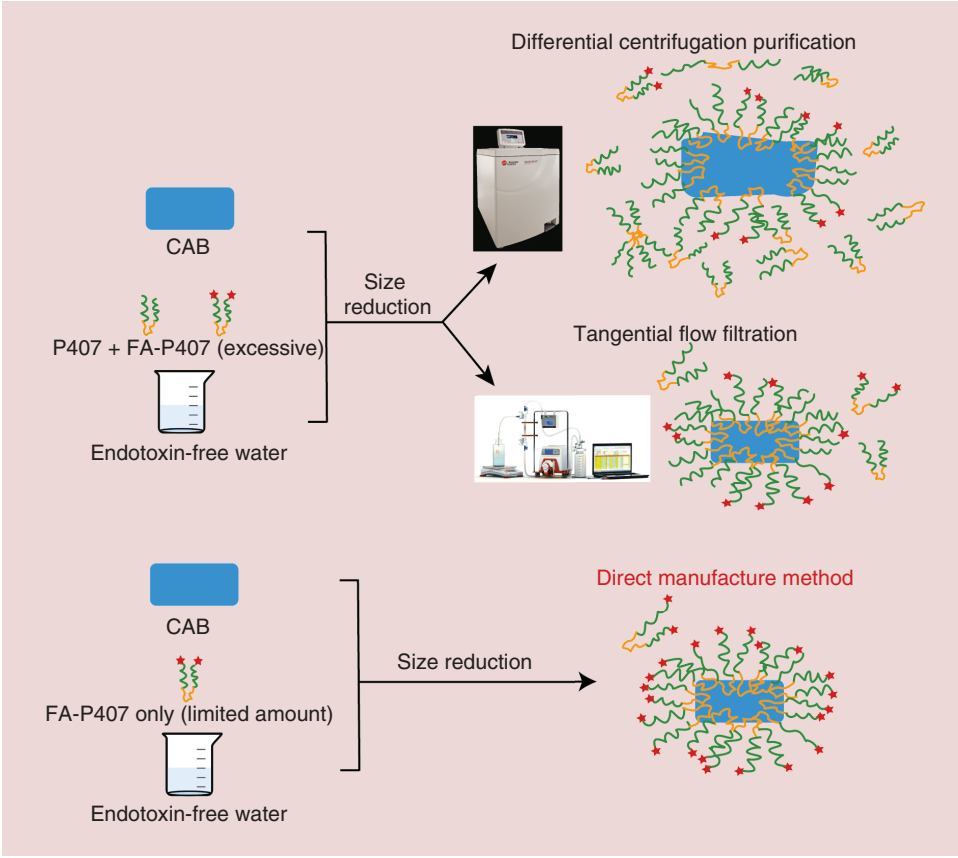

Future Medicine

Lay abstract: Folic acid (FA) decoration on the surface of nanocrystals can be achieved by mixing FA conjugated poloxamer 407 (FA-P407) and native P407 in varied ratios followed by size reduction by homogenization and differential centrifugation or tangential flow filtration to remove excess unbound polymers. The optimized manufacturing scheme is by direct homogenization with predetermined quantity of FA conjugated P407. Direct manufacturing method yields stable homogenous nanoparticles with high drug loading.

First draft submitted: 17 December 2017; Accepted for publication: 12 February 2018; Published online: 19 March 2018

Keywords: cabotegravir • long-acting antiretrovirals • monocyte-derived macrophage • nanocrystals • uptake and release

Long-acting (LA) antiretroviral therapy (ART) is being developed for the treatment and prevention of HIV infection. After parenteral injection, LA-ART provides month-long effective plasma drug concentrations overcoming obstacles in regimen adherence [1]. Notably, transition from daily oral to monthly or bimonthly injections provide consistent plasma drug concentrations and may combat drug resistance [2]. LA-ART also positively affects patient privacy by reducing social stigmas associated with daily regimens [3,4]. Indeed, LA cabotegravir (CAB) and rilpivirine (RPV), the first LA-ART combination, demonstrate comparable efficacy and safety to daily oral three drug regimens as seen, so far, in Phase II clinical trial [5]. CAB and RPV are potent antiretroviral drugs with low aqueous solubility allowing both to be formulated into 200 or 300 mg/ml wet-milled suspensions [6,7]. The formulation strategy produces pure nanosized drug crystals stabilized by surfactants with high drug loading. Nevertheless, two injections of a 2- or 3-ml volume are required to achieve desired monthly or bimonthly dosing, respectively. Injection site reactions are the most common adverse event and a reason for patient therapeutic withdrawal [5,8,9]. Variant pharmacokinetic (PK) profiles and lack of penetration into mucosal and viral reservoir tissues could also affect therapeutic outcomes and the emergence of viral resistance [6,8].

To further improve LA-ART delivery, our laboratory developed cell-targeted LA nanoformulated ART (nanoART) [10–13]. Herein, macrophages serve as 'Trojan horses' carrying crystalline ART to endosomal cell compartments [14,15]. Slow release of drug from macrophages allows for sustained drug levels thus affecting long-term viral suppression [16]. The highly mobile macrophages can also be recruited to sites of infection and inflammation [10] enabling cell cargoes to move across physiological barriers. Macrophages have a long lifespan and are less sensitive to virus-induced cytopathicity and thus readily serve as drug sanctuaries [17,18].

One means to achieve macrophage targeting is by creating ligand-targeted nanoparticles. By attaching ligands that bind to specific cell receptors, targeted nanoparticles can better reach and release therapeutic agents at the disease site. As an example, folic acid (FA) can be used as a ligand to target folate receptor-β expressed on the surface of activated macrophages [19]. Indeed, previous studies by our group have demonstrated that FA decorated nanoparticles can improve PK profiles and antiretroviral activity of ART [11,12]. FA was covalently conjugated to hydrophilic termini of amphiphilic poloxamer 407 (P407), which serves as a stabilizer to prevent aggregation of drug crystals. After high-pressure homogenization, FA conjugated P407 (FA-P407) coats the nanosized drug crystals, presenting FA on the particle surface. Excessive FA-P407 was then removed by differential centrifugation. The process is essential for targeting as unbound FA-P407 may compete with FA-decorated nanoparticles for receptor binding [11]. However, high-speed centrifugation may cause particle aggregation and limit resuspension and large-scale production. In fact, purification by differential centrifugation, filtration, dialysis or chromatography is tedious and provides limitations in the preparation of ligand-targeted formulations [20].

To address these limitations, we developed a simplified, scalable and reproducible production scheme for macrophage-targeted nanoART using CAB as a model compound. CAB is a novel highly potent integrase strand transfer inhibitor with low aqueous solubility, high melting point and protein binding and a long systemic half-life. These make CAB an excellent component of any LA-ART regimen [6]. The chemical structure of CAB is illustrated in Figure 1. The optimized manufacturing scheme obviates the need for purification. The resultant FA decorated nanoformulated CAB (FA NCAB) demonstrated high particle integrity and drug loading with potential for large-scale production. Notably, the process can be adapted to other ligand-targeted delivery systems and be of broad utility in the production of targeted drug crystals.

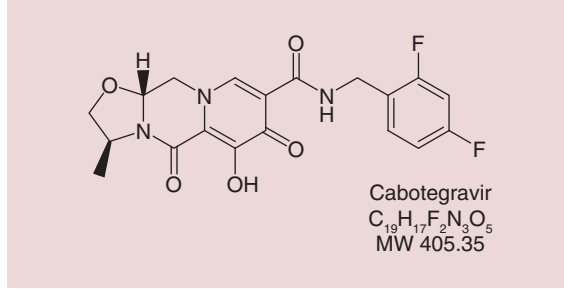

Figure 1. Chemical structure of cabotegravir. Cabotegravir is a hydrophobic integrase inhibitor under development for treatment and prevention of HIV infection. It has a long half-life of 21–50 days after a single parenteral dose.

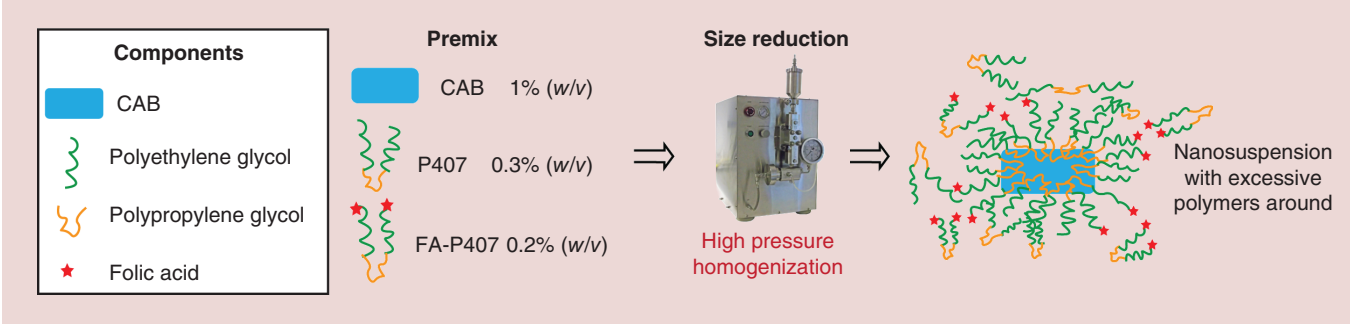

Figure 2. Size reduction scheme for folic acid nanoformulated cabotegravir. 1% (*w*/*v*) cabotegravir was dispersed in polymer solutioncontaining both targeted and nontargeted P407 polymer, followed by high-pressure homogenization until the desired particle size and polydispersity index was achieved. The size-reduced particles contained excessive polymers and needed further purification. CAB: Cabotegravir; FA: Folic acid; FA-P407: FA conjugated poloxamer 407; P407: Poloxamer 407.

Materials & methods

Materials

CAB and CAB LA parenteral (CAB-LAP) were a gift from ViiV Healthcare (NC, USA). P407, poloxamer 188, PEG 2000, PEG 3350, PEG 4600, histidine, sodium carboxymethyl cellulose, sucrose, dextrose, trehalose, glucose and mannitol were purchased from Sigma-Aldrich (MO, USA). FA-P407 was synthesized as previously described [11]. Dulbecco's modified eagle's medium was purchased from Corning Life Sciences (MA, USA). Heat-inactivated pooled human serum was obtained from Innovative Biologics (VA, USA). Gentamicin, HPLC grade acetonitrile, HPLC grade methanol and Optima grade liquid chromatography–mass spectrometry (LC/MS) water were purchased from Thermo Fisher Scientific (MA, USA).

High-pressure homogenization

For preparation of multistep purified formulations, 1% (*w*/*v*) CAB was added to a solution of 0.3% (*w*/*v*) P407 and 0.2% (*w*/*v*) FA-P407 in endotoxin-free water (Figure 2). For optimized direct preparation, 5% (*w*/*v*) CAB was premixed with 0.15% (*w*/*v*) FA-P407 solution. Polymer stabilized drug suspensions were stirred on a magnetic stir plate for at least 16 h at room temperature followed by high-pressure homogenization (Avestin EmulsiFlex-C3; Avestin, Inc., Ottawa, ON, Canada) at 20,000 psi to a desired particle size of approximately 300 nm.

Differential centrifugation

After homogenization, the nanosuspensions were purified by sequential centrifugations. The suspension was first centrifuged at 10,000 × *g* for 15 min. The supernatant was discarded and the pellet resuspended in 0.2% (*w*/*v*) P407. The redispersed nanoparticles were then centrifuged at 200 × *g* for 1 min to remove poorly dispersed particles. Supernatant from the secondary centrifugation was collected as the final formulation.

Tangential flow filtration

To remove excessive polymer, homogenized suspensions were diafiltrated using a Kros Flo research IIi tangential flow filtration (TFF) system (Spectrum Laboratories, Inc., CA, USA) with a mPES MidiKros® Filter Module

(cut-off size: 0.2 µm; surface area: 20 cm^2). For a 15 ml suspension, the formulation was concentrated to 5 ml followed by diafiltration with 5 or 10 diavolumes (DV) of water.

Physicochemical characterizations

Effective diameter (D_{eff}), polydispersity index (PdI), and ζ-potential of the nanoformulations were assessed by dynamic light scattering using a Malvern Zetasizer Nano Series Nano-ZS (Malvern Instruments, Inc., MA, USA). Encapsulation efficiencies of the formulations were calculated using the following equation:

$$\text{Encapsulation efficiency (\%)} = \frac{\text{weight of drug in formulation}}{\text{weight of drug fed initially}} \times 100$$

The morphologies of nanoformulations were examined by scanning electron microscopy (SEM) using a Hitachi S4700 field-emission scanning electron microscope (Hitachi High Technologies America, Inc., IL, USA). Proton nuclear magnetic resonance (^{1}H-NMR) spectroscopy was used to analyze the structure and drug-to-polymer ratio in the FA NCAB formulation.

Stability measurements

Stabilities of formulations prepared by the described manufacturing methods were assessed after prolonged storage at 4°C. D_{eff}, PdI and ζ-potential were measured at predetermined times to assess particle integrity. The formulations were considered unstable when D_{eff} reached >500 nm and or the PdI was >0.3.

Monocyte-derived macrophages

Human peripheral blood monocytes were obtained and cultured as described [21]. Briefly, peripheral blood monocytes were obtained by leukapheresis from HIV-1/2 and hepatitis B seronegative donors and purified by countercurrent centrifugal elutriation. Monocytes were cultured in Dulbecco's modified eagle's medium supplemented with 10% heat-inactivated pooled human serum, 10 µg/ml ciprofloxacin, 50 µg/ml gentamicin and 1000 U/ml recombinant macrophage colony-stimulating factor for 7 days to promote differentiation into macrophages. Macrophages were treated with 100 µM CAB nanoformulations. At predetermined time points, monocyte-derived macrophages (MDM) were washed three-times with sterile phosphate-buffered saline (PBS) and scraped into 1 ml PBS. Cell pellets were collected by centrifugation at 1000 × *g* for 8 min, followed by probe sonication in 200 µl of HPLC grade methanol to extract CAB. CAB concentrations were determined using a Waters ACQUITY ultra performance liquid chromatography (UPLC) H-Class System with TUV detector and Empower 3 software (Milford, MA, USA) [22].

PK tests

Male BALB/cJ mice (Jackson Labs, ME, USA) were dosed intramuscularly with 45 mg/kg FA NCAB purified by TFF or prepared directly. CAB-LAP was used as a nontargeted control. Blood was collected at days 3, 7, 14, 21 and 28 into heparinized tubes and plasma prepared by centrifugation at 2000 × *g* for 5 min. At day 28 after nanoART administration, mice were sacrificed and liver, spleen and lymph nodes were collected after whole body perfusion with PBS. Plasma and tissue CAB concentrations were measured by UPLC tandem mass spectrometry (UPLC–MS/MS) as previously described [22]. Noncompartmental PK analysis for plasma CAB was performed using WinNonlin-5.1 (Certara USA, Inc., NJ, USA).

Results

Particle size reductions

A general scheme designed for particle size reduction is illustrated in Figure 2. FA NCAB is produced by premixing CAB (1% *w*/*v*) with a P407 (0.3% *w*/*v*) and FA-P407 (0.2% *w*/*v*) solution using a magnetic stir bar. Premixing suspends and disintegrates drug crystals to prevent clogging of the homogenizer. High-pressure homogenization further reduced particle size (D_{eff}) to approximately 300 nm with a narrow PdI of 0.228 and negative surface charge (Table 1, before purification).

Table 1. Folic acid-decorated nanoformulated cabotegravir physicochemical properties.

Method	Purification	D_{eff} (nm)	PdI	ζ-potential (mV)
Differential centrifugation	-	312 ± 3	0.228 ± 0.013	-30.5 ± 1.2
	+	454 ± 5	0.180 ± 0.029	-22.1 ± 0.4
TFF	-	290 ± 2	0.263 ± 0.013	-29.0 ± 0.4
	+ (5 DV)	285 ± 4	0.258 ± 0.019	-28.6 ± 0.8
	+ (10 DV)	295 ± 2	0.267 ± 0.016	-22.5 ± 0.3
Direct preparation	-	319 ± 5	0.277 ± 0.041	-37.8 ± 1.9

DV: Diavolume; PdI: Polydispersity index; TFF: Tangential flow filtration.

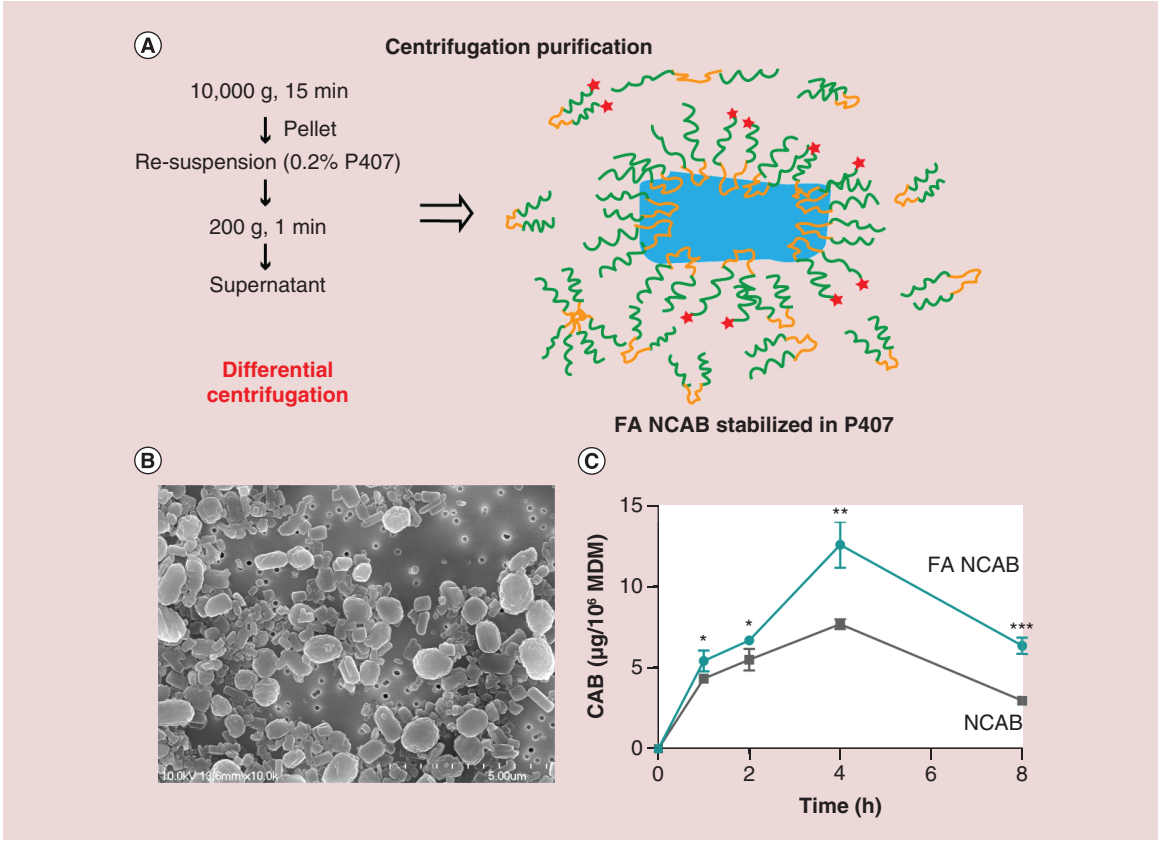

Figure 3. Folic acid nanoformulated cabotegravir preparations purified by differential centrifugation. (A) Post homogenization process scheme of FA NCAB purified by differential centrifugation. High speed centrifugation at 10,000 × *g* was used to pellet FA NCAB followed by resuspension in 0.2% (*w*/*v*) P407 solution. Large particles that cannot disperse during resuspension were removed by low speed centrifugation at 200 ×*g*. **(B)** Morphology of FA NCAB purified by centrifugation was visualized by scanning electron microscopy. Scale bar: 5 µm. **(C)** Cellular uptake of FA NCAB prepared by differential centrifugation was assessed in human MDM and compared with nanoformulation without targeting ligand (NCAB). Intracellular drug concentrations were determined in MDM treated with 100 µM NCAB or FA NCAB for 1–8 h. Intracellular drug concentrations were analyzed by HPLC-UV/vis. Data are expressed as mean ± standard deviation for n = 3 samples per group. For each time point, means were compared by two-tailed Student's t-test.
*$p < 0.05$; **$p < 0.01$; ***$p < 0.001$.
CAB: Cabotegravir; FA NCAB: Folic acid decorated nanoformulated CAB; FA-P407: FA conjugated poloxamer 407; MDM: Monocyte-derived macrophage; P407: Poloxamer 407.

FA NCAB purification by differential centrifugation

To remove unbound FA-P407 that could compete for receptor binding, differential centrifugation was used. The process involves high-speed centrifugation, followed by redispersion of the pellet in a P407 solution (Figure 3A). A total of 30% of the drug is lost during this process, yielding an encapsulation efficiency of 72%. Additionally,

centrifugation resulted in an increased D_{eff} from 312 to 454 nm coupled with a reduced surface charge (Table 1). The size increase was due to formation of aggregates that were readily observed by SEM (Figure 3B). Despite increased particle size, FA NCAB maintained its targeting ability. As shown in Figure 3C, FA NCAB treatment resulted in approximately twofold greater drug concentration in MDM compared with a parallel NCAB formulation without FA-P407. The highest drug concentration was observed 4 h after treatment for FA NCAB (12.5 μg/10^6 MDM) and NCAB (7.8 μg/10^6 MDM) after which drug concentration decreased.

FA NCAB preparation by TFF

To preclude particle aggregation caused by high-speed centrifugation, the efficiency of TFF to remove unbound FA-P407 was evaluated (Figure 4A). Both 5 and 10 DV of water were used for diafiltration. The D_{eff} and PdI of FA NCAB nanoparticles were not altered after TFF purification (Table 1). Encapsulation efficiencies of nanoparticles subjected to 5 or 10 DV were 78.2 and 70.4%, respectively. The TFF purified formulations (both 5 and 10 DV) remained stable in terms of D_{eff}, PdI and ζ-potential without additional stabilizers for at least one month (Figure 4B). TFF-purified FA NCAB nanoparticles were homogeneous with more cuboidal morphologies when compared with those purified by differential centrifugation (Figure 4C). The targeting ability of the particles was maintained after TFF purification. MDM uptake was two- to three-fold greater for TFF-purified FA NCAB compared with nontargeted formulations (Figure 4D).

Direct manufacture

Having successfully produced stabilizer-free TFF-purified FA NCAB nanoparticles, we determined the polymer content of the nanoparticles to facilitate development of a simplified direct manufacturing scheme for ligand-targeted nanoformulations to bypass the need for purification. TFF-purified FA NCAB was lyophilized and drug-to-polymer ratios were determined by evaluation of integral areas in the ^{1}H-NMR spectrum. As shown in Figure 5, the peak labeled 'A' with a chemical shift at 5.36 p.p.m. corresponds to a single proton from CAB, while peak 'B' corresponds to 930 protons from the PEG and polypropylene glycol repeating units of P407. The CAB to P407 ratio (*w*/w) for TFF-purified formulations was calculated based on integral values of the assigned protons in the spectrum. To optimize the calculated ratios, variant drug-to-polymer ratios within the range of 16:1–45:1 were evaluated. FA NCAB prepared directly are protected against mechanical stresses such as centrifugation or TFF that could damage the particle. Direct manufacturing also permits high drug loading without compromising particle integrity. High-pressure homogenization then achieved a stable particle size and narrow PdI for nanocrystals containing up to 20% (*w*/*v*) CAB (data not shown).

The optimized formulation procedure is illustrated in Figure 6A. Pure FA-P407 was used at a drug-to-polymer ratio of 100:3. Directly prepared FA NCAB was stable for up to 80 days by D_{eff}, PdI and ζ-potential measurements. Thereafter, nanoparticle size began to increase (Figure 6B). Direct preparation of nanoparticles also resulted in uniform morphologies (Figure 6C). The elimination of posthomogenization purification steps resulted in a ≥99% encapsulation efficiency. Targeting ability of the produced formulation was confirmed by MDM uptake wherein FA NCAB treatment resulted in intracellular CAB concentrations of 7.8 μg/10^6 cells at 4 h, which was approximately fourfold higher than in NCAB treated cells (2.0 μg/10^6 cells; Figure 6D). In the presence of free FA, FA NCAB uptake by MDM was reduced to levels comparable to NCAB control. Cellular drug concentration was 2.6 μg/10^6 cells when co-incubated with 25 mM free FA for 4 h (Figure 6E).

PK evaluation

Male BALB/cJ mice were administered a single intramuscular FA NCAB injection at 45 mg/kg. These were prepared by either TFF or direct preparation for PK and biodistribution drug measures. A total of 14 days after injection, animals treated with FA NCAB made by either TFF or direct methods showed higher plasma CAB concentrations (22,050 and 22,780 ng/ml, respectively) when compared with CAB-LAP (15,250 ng/ml). Direct FA NCAB manufacture led to sustained plasma drug levels over the 28-day study (14,400 ng/ml). In contrast, the TFF purified formulation showed a faster decay. Indeed, at 28 days the plasma drug concentration (3679 ng/ml) was comparable to that of animals administered CAB-LAP (3125 ng/ml; Figure 7A). Noncompartmental PK analysis was performed for all the formulations (Table 2). Direct FA NCAB preparations resulted in a threefold longer apparent terminal phase half-life ($t_{1/2}$) compared with CAB-LAP (22.3 vs 6.9 days, respectively), while TFF-prepared FA NCAB did not exhibit any significant improvement ($t_{1/2}$ of 7.7 days) compared with CAB-LAP. Similarly, the volume of distribution (Vβ/F) increased, while clearance (CL/F) was reduced in mice given direct

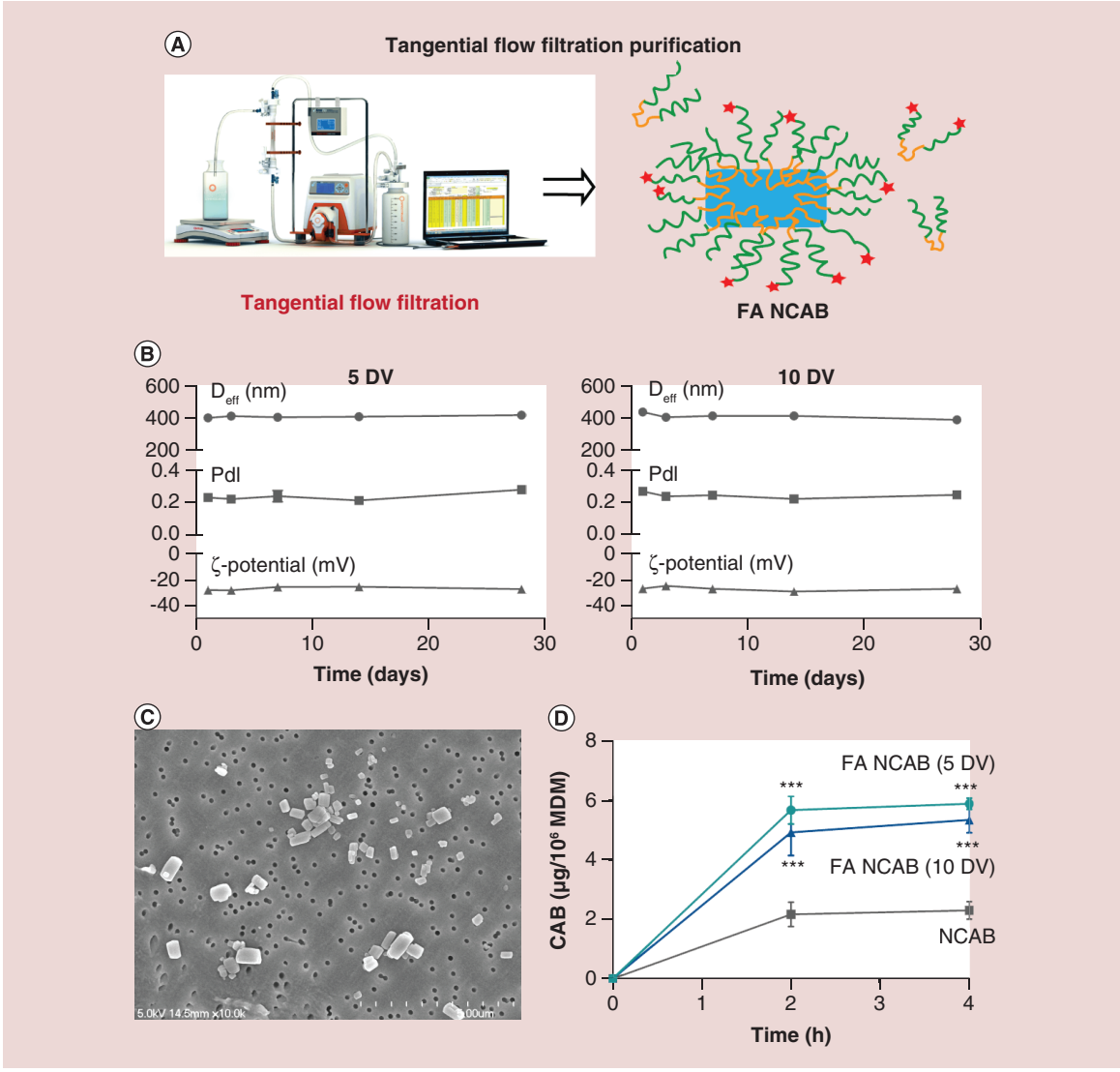

Figure 4. Folic acid decorated nanoformulated cabotegravir preparations by tangential flow filtration. (A) Manufacturing scheme for FA NCAB purified by tangential flow filtration (TFF). FA NCAB was purified by TFF diafiltration using 5 or 10 DV of water. **(B)** Time course measurements of FA NCAB prepared by TFF for Deff, ζ-potential and polydispersity index. Data are expressed as mean ± standard deviation for n = 3 measurements. **(C)** Morphology of FA NCAB purified by TFF was visualized by scanning electron microscopy. Scale bar: 5 µm. **(D)** Cellular uptake of FA NCAB prepared by TFF was assessed in human MDM and compared with formulation without targeting ligand or NCAB. Intracellular drug concentrations were determined in MDM treated with 100 µM NCAB or FA NCAB for 2 and 4 h. Intracellular drug concentrations were analyzed by HPLC-UV/vis. Data are expressed as mean ± standard deviation for n = 3 samples per group. One-way ANOVA followed by Tukey's *post hoc* test was used to compare FA NCAB with nontargeted NCAB formulation.
***$p < 0.001$.
CAB: Cabotegravir; DV: Diavolume; FA NCAB: Folic acid decorated nanoformulated cabotegravir; MDM: Monocyte-derived macrophage; PdI: Polydispersity index.

preparations of FA NCAB. Drug levels in liver, spleen and lymph nodes at day 28 correlated with the plasma drug concentrations. Notably, directly prepared FA NCAB resulted in higher tissue drug concentrations compared with treatment with FA NCAB produced using TFF or CAB-LAP (Figure 7B).

Additives

To adjust tonicity and further stabilize the formulation from direct method, we examined a variety of buffers, stabilizers and tonicity adjusters (Table 3). Salts, including phosphate buffer, PBS, HEPES, histidine and sodium

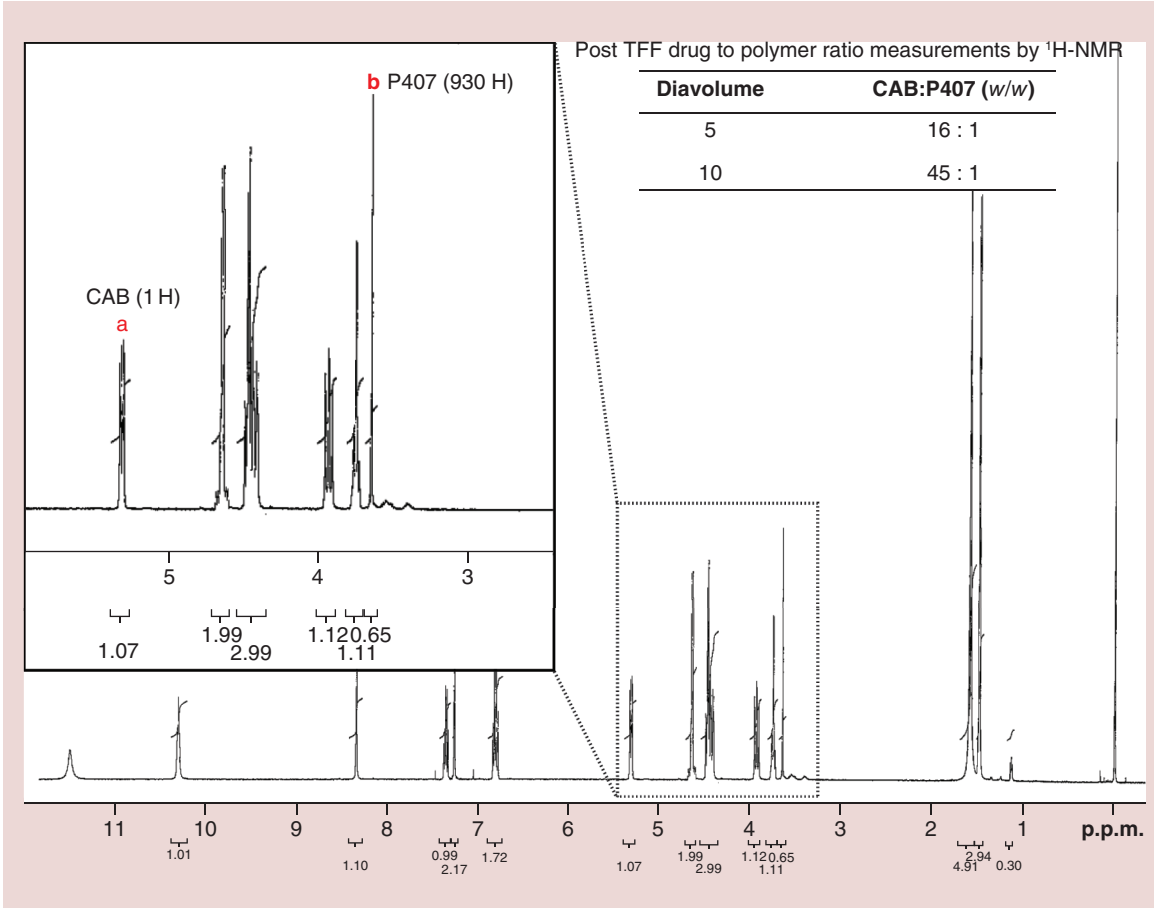

Figure 5. Proton nuclear magnetic resonance spectrum of lyophilized folic acid decorated nanoformulated cabotegravir formulation purified by tangential flow filtration. Drug to P407 ratio was calculated based on characteristic integral peak areas of CAB and P407.
CAB: Cabotegravir; ^{1}H-NMR: Proton nuclear magnetic resonance; P407: Poloxamer 407; TFF: Tangential flow filtration.

Table 2. Noncompartmental pharmacokinetic analysis.

PK parameters	CAB-LAP	FA NCAB (direct)	FA NCAB (TFF)
λZ (1/day)	0.100	0.031	0.090
$t_{1/2}$ (day)	6.9	22.3	7.7
AUC_{last} (day*ng/ml)	546,640.6	726,640.0	650,934.0
$AUC_{0-\infty}$ (day*ng/ml)	577,934.2	1,189,658.7	691,786.8
AUC % extrapolation	5.41	38.92	5.91
Vβ/F (l/kg)	0.78	1.22	0.72
CL/F (l/day/kg)	0.08	0.04	0.07
MRT $_{0-\infty}$ (days)	11.1	32.8	12.5

AUC: Area under the curve; CAB-LAP: Cabotegravir long-acting parenteral; FA NCAB: Folic acid decorated nanoformulated cabotegravir; MRT: Mean residence time; PK: Pharmacokinetic; TFF: Tangential flow filtration; Vβ/F: Volume of distribution.

carboxymethyl cellulose, decreased FA NCAB stability resulting in a greater than 50% increase in D_{eff} to over 500 nm. For instance, addition of 0.2% (*w*/*v*) sodium carboxymethyl cellulose to FA NCAB particles increased the size from 300 to 1042 nm with a broad size distribution (PdI >0.5). Histidine buffer caused a gradual incremental increase in particle size. Seven days after particle preparation, the D_{eff} was 688 nm with a PdI of 0.296. Sugars, including sucrose, dextrose, trehalose, glucose and mannitol, elicited a stable particle size and PdI for 1 month or longer. PEG 3350 is one of the excipients in the CAB-LAP formulation [6]. Thus, PEGs of various molecular weights

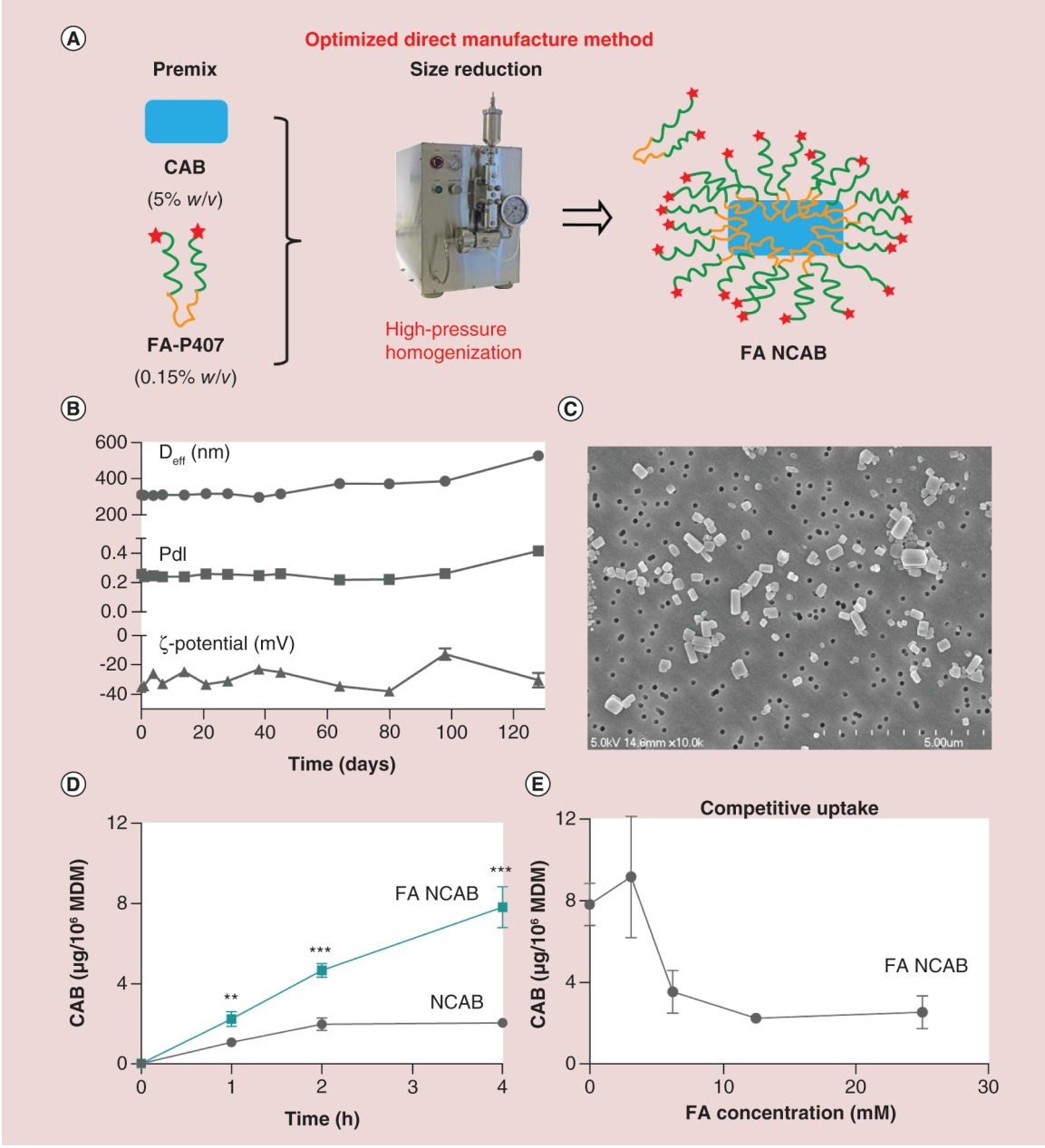

Figure 6. Direct preparation of folic acid decorated nanoformulated cabotegravir. (A) Manufacturing scheme of FA NCAB prepared by a direct method. **(B)** Time course measurements of direct prepared FA NCAB over 120 days for Deff, ζ-potential and polydispersity index. Data are expressed as mean ± standard deviation (SD) for n = 3 measurements. **(C)** Morphology of FA NCAB prepared by the direct method was visualized by scanning electron microscopy. Scale bar: 5 µm. **(D)** Monocyte-derived macrophage (MDM) uptake of NCAB and FA NCAB prepared by the direct method. MDM were treated with 100 µM NCAB or FA NCAB, and intracellular drug concentrations were analyzed by HPLC-UV/vis at 1, 2 and 4 h after drug treatment. Data are expressed as mean ± SD for n = 3 samples. For each time point, means were compared by two-tailed Student's t-test. **$p < 0.01$; ***$p < 0.001$. **(E)** Competitive uptake study of FA NCAB. Cells were pretreated with free FA (0–25 mM) for 30 min to block folate receptors, followed by FA NCAB treatment. Data are expressed as mean ± SD for n = 3 samples.
CAB: Cabotegravir; FA: Folic acid; FA NCAB: Folic acid decorated nanoformulated cabotegravir; FA-P407: FA conjugated poloxamer 407; PdI: Polydispersity index.

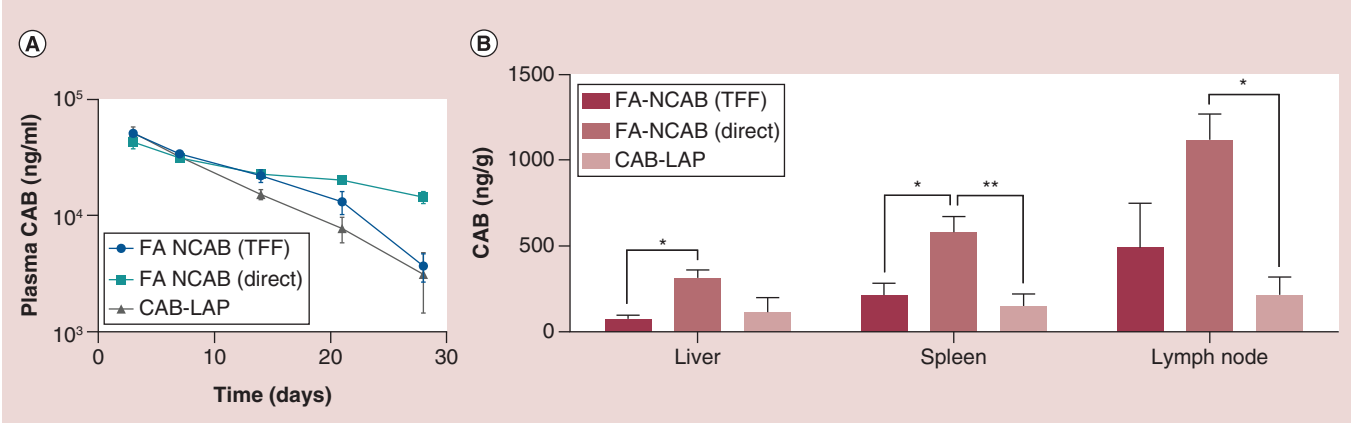

Figure 7. Folic acid decorated nanoformulated cabotegravir pharmacokinetic and biodistribution profiles. Male BALB/cJ mice were administered intramuscularly 45 mg/kg FA NCAB purified by TFF or directly prepared to 45 mg/kg CAB-long-acting parenteral treatment. **(A)** Plasma was collected at days 3, 7, 14, 21 and 28 after drug administration and CAB concentrations were determined by ultra performance liquid chromatography tandem mass spectrometry. Data represent mean ± standard error of the mean for n = 5 mice per group. **(B)** Tissues were collected at day 28 and CAB concentrations were determined by ultra performance liquid chromatography tandem mass spectrometry. Data are expressed as mean ± standard error of the mean for n = 5 mice per group. Tissue CAB concentrations were compared by one-way ANOVA followed by Tukey's *post hoc* test.
*$p < 0.05$; **$p < 0.01$.
CAB: Cabotegravir; CAB-LAP: Cabotegravir long-acting parenteral; FA NCAB: Folic acid decorated nanoformulated cabotegravir; TFF: Tangential flow filtration.

Table 3. The effect of additives on folic acid decorated NCAB stability.

Excipients	Concentration (%)	pH	Formulation stability (weeks)†
Phosphate buffer	–	6.8	0
PBS	–	6.8	0
HEPES buffer	10 mM	6.8	0
Histidine	0.2 (*w*/*v*)	6.8	1
Sodium carboxymethyl cellulose	0.2 (*w*/*v*)	NA	0
Sucrose	0.2; 1; 2 (*w*/*v*)	NA	>4
Dextrose	0.2; 1; 2 (*w*/*v*)	NA	>4
Trehalose	0.2; 1; 2 (*w*/*v*)	NA	>4
Glucose	0.5 (*w*/*v*)	NA	9
Mannitol	0.5 (*w*/*v*)	NA	8
PEG 2000	0.5 (*w*/*v*)	NA	>3
PEG 3350	0.5 (*w*/*v*)	NA	>3
PEG 4600	0.5 (*w*/*v*)	NA	1
P407	0.5 (*w*/*v*)	NA	>3
P188	0.5 (*w*/*v*)	NA	>3

†The formulations were considered to be unstable when D_{eff} > 500 nm and/or polydispersity index > 0.03.
NA: Not applicable; P188: Poloxamer 188; P407: Poloxamer 407; PBS: Phosphate-buffered saline.

were also screened. PEG 2000 and 3350 were compatible with FA NCAB while the high molecular weight PEG 4600 resulted in a particle size increase to over 500 nm 1 week after preparation. Additional P407 and poloxamer 188 did not affect the stability of FA NCAB. Mannitol and glucose were selected for further stability evaluation under variable temperature conditions. As shown in Supplementary Figure 1, without additives FA NCAB was stable at 63 days at 4, 25 and 37°C. In the presence of 0.5% (*w*/*v*) glucose, D_{eff} increased from 350 to 378 nm, 381 and 483 nm at 4, 25 and 37°C, respectively, by day 63. Storage at 37°C also resulted in a PdI of more than 0.3 after day 49. Additional mannitol was able to maintain a stable D_{eff} and PdI for 35 and 56 days when stored at 4 and 25°C, respectively. At 37°C, there was a slight increase in D_{eff} at day 3 to approximately 390 nm, which

remained stable afterward. Based on these data sets, glucose yielded stable FA NCAB compared with mannitol. Macrophage uptake measurements (Supplementary Figure 2) demonstrated that additional mannitol or glucose did not affect particle cell entry.

Discussion

LA medicines show promise in achieving improved therapeutic outcomes for HIV/AIDS. Prolonged dosing intervals and less fluctuation in plasma drug concentrations can result in improved regimen adherence, reductions in systemic toxicities, reduced viral mutations and reduced HIV stigma related to observed use of daily ART [1,23]. To meet the needs of global increases in the numbers of infected people, innovative robust and scalable formulation processes and devices are of immediate need [23–27]. A successful drug-delivery scheme requires high drug encapsulation and loading that would maintain sufficient amount of drug for months within a suitable injection volume. Emerging trends in drug-delivery systems rely on the use of nanocrystals to facilitate dissolution and delivery of hydrophobic drugs [28]. Nanocrystals are composed of 100% nanosized drug crystals stabilized by aqueous surfactant solutions, thus circumvent organic solvent related side effects. The resultant high drug loading and drug-to-excipient ratios limit incompatibility and toxic reactions linked to excipients [29]. Process equipment is readily available for current pharmaceutical industry enabling batch to batch reproducibility and ease of scale-up production [30]. In current practice, RPV and CAB-LA formulations are nanocrystals manufactured by wet milling, a commonly used top-down technology for hydrophobic drug crystal manufacture. In this method, coarse drug powder is predispersed in an aqueous surfactant solution and then size-reduced by milling beads under agitation. Surfactants such as polysorbate 20 (for CAB) and poloxamer 338 (for RPV) [6,7] are used to wet the coarse powder and prevent the resultant nanoparticles from aggregation. Preparation of nanoparticles by wet milling is dependent on the target particle size and drug concentration and is completed after hours to days. For FA NCAB formulation, high-pressure homogenization was used *in lieu* of milling. It is also a top-down method. Nonionic poloxamers are adsorbed on the surface of nanocrystals to prevent nanoparticle aggregation during storage and administration [29,30].

The ideal delivery systems must both protect the drug cargo against degradation then deliver it to sites of active viral replication. To facilitate targeted delivery, FA decorations were introduced to enhance particle uptake into macrophages. Macrophages are a target cell and reservoir for HIV [31,32] but can also serve as nanocrystal drug depots [15]. Indeed, because of their phagocytic functions, macrophages can serve as drug-delivery vehicles. Their intrinsic high mobility allows the cells to readily cross physiological barriers to sites of infection. Thus, drug cargoes can easily access sites of viral growth, such as the gut-associated lymphoid tissue, brain and lymph nodes, employing macrophages as the principal drug transporter [13,33]. Furthermore, depending on surface chemistry and lipophilic properties, nanoparticles phagocytosed by macrophages can be disseminated from vesicles in the cytoplasm into the surrounding tissues and other cell types [34]. This depot effect could result in reduced maximal plasma drug concentration (C_{max}) and prolonged apparent half-life ($t_{1/2}$), which could potentially reduce drug dose and high peak drug concentration-induced toxicities, while extending dosing intervals [29].

Prior studies performed by our group demonstrated that FA-decorated ART particles enhance delivery to tissue macrophages [10–12,34–36]. FA was conjugated to hydrophilic termini of P407 and coated on the surface of nanocrystals to gain entry into the cell through the folate receptor-β expressed on the surface of activated macrophages [19]. One apparent hurdle for translation to clinical use is the complexity of the formulation process when a targeting ligand is introduced. Active targeting not only requires presentation of the ligand on the surface of the formed particles to interact with cell surface receptors, but also the amount of targeting ligand and orientation is critical for rapid internalization of the drug loaded particles. Standard purification steps such as differential centrifugation, dialysis and filtration are often required to remove unbound targeted polymers that could compete for receptor binding. However, these processes are usually time consuming and the additional force during purification could destabilize adsorbed surfactants to form particle aggregates and/or loss of targeting ability. Indeed, particle aggregation was observed when differential centrifugation was used to purify the FA NCAB formulation. Large-sized particles obtained by centrifugation were rapidly taken up by macrophages compared with smaller sized homogeneous nanocrystals from direct or TFF preparation methods. Numerous studies have shown that macrophages have a higher phagocytic activity toward microparticles than nanoparticles [37]. However, aggregation and poor homogeneity of microparticles could potentially affect drug release resulting in uneven plasma drug levels and unpredictable PK profiles after administration.

To overcome nanoparticle purification limitations of high-speed centrifugation, a mild but effective TFF method was tested. After diafiltration, the resultant FA NCAB formulation was stable in terms of particle size, size

distribution and surface charge. Notably, particle stability did not rely on additional surfactants or stabilizers. NMR spectroscopy was then used to determine drug-to-polymer ratios in the nanoparticles after TFF purification to facilitate development of a direct method for targeted formulations. The resultant manufacturing scheme was simple and scalable with no purification steps. It is also worth noting that the TFF scheme utilizes a premix of folate modified and nontargeted P407 surfactants to stabilize nanoparticles, while the direct method incorporates limited amounts of the folate modified polymer alone. Most importantly, FA NCAB nanocrystals from the direct scheme retained macrophage targeting ability. Of particular note, an improved PK profile was observed for FA NCAB nanocrystals produced by the direct scheme over those processed by TFF. Diafiltrated particles provided limited improvement over the nontargeted CAB-LAP formulation. This is most likely linked to continuous polymer exchange on the particle surface. In contrast, optimized FA NCAB was directly prepared with pure targeted polymer, and therefore polymer exchange would not affect its targeting ability. Because only a limited amount of polymer was used, tonicity adjusters and stabilizers may still be required for injection and long-term storage. Salts were found to be incompatible with the FA NCAB formulation, likely due to electrostatic interactions with the drug or polymer that would disrupt the nanoparticle surface. Sugars such as glucose and mannitol, in contrast, maintained FA NCAB stability for a long period of time.

Taken together, while current LA-ART nanoformulations demonstrate considerable potential for HIV treatment and prevention, further drug formulation refinements would improve intracellular and tissue drug delivery profiles and as such maximally affect viral restriction [16,24,38,39]. The current report demonstrating improvements in the manufacturing scheme for ligand-targeted nanocrystals is a notable step forward in development of the next generation of LA-ART for human use.

Conclusion

LA macrophage-targeted FA-decorated CAB nanocrystals were successfully prepared with stable profiles. The FA NCAB particles displayed enhanced uptake by macrophages compared with nontargeted particles. We successfully simplified formulation preparation for targeted drug nanocrystals. The resultant manufacturing scheme enabled direct preparation of targeting ligand-decorated nanocrystals. Such improvements obviated complex purification steps. With improved PK profiles, FA NCAB has a real translational potential for inclusion in future HIV management schemes.

Future perspective

Despite promising results for LA-ART, challenges remain to further ease formulation administration and to restrict injection site adverse effects. Discovery of novel highly potent antiretroviral drugs to lower the overall required dose is one path. Alternatively, formulation strategies such as co-formulation of multiple drugs in a single delivery system or reduction of unnecessary excipient usage as reported in this report could further ease drug regimen administration for broader application. Another concern for LA-ART is that once injected, the regimen cannot be removed, which could potentially expose patients to intractable adverse effects. One solution is the use of oral lead-in regimens of the same drugs as currently applied in clinical trials [5]. Development of retrievable LA-ART will also provide a solution. Nevertheless, current retrievable LA-ART requires procedures to insert or retrieve the implantable agents [40], which could be a concern for patients and may need additional infrastructure. Therefore, retrievable LA-ART that can be easily administered could further broaden the application of LA-ART. Also, with the technical hurdles addressed, the next generation of LA-ART can target specific receptors using a readily translatable manufacturing process. Various targeting ligands, such as hyaluronic acid [41], tuftsin [42], gp120 peptide [43,44], etc., can be tested using this manufacturing scheme. Such targeting strategies could result in further prolonged dosing intervals, effective drug concentrations within viral reservoir tissues and reduced systemic toxicities, which will positively affect ART and prevention outcomes.

Supplementary data

To view the supplementary data that accompany this paper please visit the journal website at: www.futuremedicine.com/doi/suppl/10.2217/nnm-2017-0381.

Author contributions

HE Gendelman, B Edagwa and T Zhou designed the research. B Edagwa, X Liu and T Zhou synthesized and characterized the FA-P407. T Zhou and Z Lin performed formulation screening and characterization. T Zhou and P Puligujja prepared and characterized

Summary points

- Folic acid-decorated nanoformulated cabotegravir prepared by differential centrifugation had particle aggregation and reproducibility problems that are not suitable for large-scale production.
- Tangential flow filtration purification was able to maintain particle morphology, whereas the targeting ability was compromised.
- Folic acid decorated nanoformulated cabotegravir was successfully manufactured using a direct method and demonstrated appreciable particle stability and reproducibility in cellular uptake and pharmacokinetic profiles.

formulation by differential centrifugation. T Zhou executed cellular uptake study. T Zhou, Z Lin, J Hilaire, M Araínga and J McMillan designed and performed pharmacokinetics study in mice. N Smith, N Gautam and Y Alnouti developed UPLC–MS/MS method for drug concentration analysis. D Palandri processed plasma and tissue samples for UPLC–MS/MS analysis. HE Gendelman, B Edagwa and T Zhou wrote the manuscript. HE Gendelman provided funding support and overall scientific direction for the studies.

Acknowledgements

We wish to thank M Che, L Wu and N Ly of the University of Nebraska Medical Center Research Core (NE, USA) for elutriation. We thank Z You of the University of Nebraska-Lincoln Center for Biotechnology (NE, USA) for scanning electron microscope analysis.

Financial & competing interests disclosure

This work was supported by ViiV Healthcare and National Institutes of Health Grants AG043540, DA028555, NS036126, NS034239, MH064570, NS043985 and MH062261, the Carol Swarts Emerging Neuroscience Fund and the Nebraska Research Initiative. The authors have no relevant affiliations or financial involvement with any organization or entity with a financial interest in or financial conflict with the subject matter or materials discussed in the manuscript apart from those disclosed.

No writing assistance was utilized in the preparation of this manuscript.

Ethical disclosure

The authors have obtained appropriate institutional review board approval and followed the principles outlined in the Declaration of Helsinki for all human or animal experimental investigations. Specifically, all animal studies were conducted under a protocol approved by the University of Nebraska Institutional Animal Care and Use Committee in accordance with the standards incorporated in the Guide for the Care and Use of Laboratory Animals (National Research Council of the National Academies, 2011).

References

Papers of special note have been highlighted as: • of interest; •• of considerable interest

1. Dolgin E. Long-acting HIV drugs advanced to overcome adherence challenge. *Nat. Med.* 20(4), 323–324 (2014).
2. Hickey MB, Merisko-Liversidge E, Remenar JF, Namchuk M. Delivery of long-acting injectable antivirals: best approaches and recent advances. *Curr. Opin. Infect. Dis.* 28(6), 603–610 (2015).
3. Carrasco MA, Arias R, Figueroa ME. The multidimensional nature of HIV stigma: evidence from Mozambique. *Afr. J. AIDS Res.* 16(1), 11–18 (2017).
4. Sangaramoorthy T, Jamison AM, Dyer TV. HIV stigma, retention in care, and adherence among older black women living with HIV. *J. Assoc. Nurses AIDS Care* 28(4), 518–531 (2017).
5. Margolis DA, Gonzalez-Garcia J, Stellbrink H-J *et al.* Long-acting intramuscular cabotegravir and rilpivirine in adults with HIV-1 infection (LATTE-2): 96-week results of a randomised, open-label, Phase IIB, non-inferiority trial. *Lancet* 390(10101), 1499–1510 (2017).

• **Long-acting cabotegravir plus rilpivirine Phase II clinical study for maintenance therapy.**

6. Trezza C, Ford SL, Spreen W, Pan R, Piscitelli S. Formulation and pharmacology of long-acting cabotegravir. *Curr. Opin. HIV AIDS* 10(4), 239–245 (2015).
7. Williams PE, Crauwels HM, Basstanie ED. Formulation and pharmacology of long-acting rilpivirine. *Curr. Opin. HIV AIDS* 10(4), 233–238 (2015).

8. Markowitz M, Frank I, Grant RM *et al.* Safety and tolerability of long-acting cabotegravir injections in HIV-uninfected men (ECLAIR): a multicentre, double-blind, randomised, placebo-controlled, Phase IIA trial. *Lancet HIV* 4(8), e331–e340 (2017).

• **Long-acting cabotegravir as pre-exposure prophylaxis for HIV prevention.**

9. McGowan I, Dezzutti CS, Siegel A *et al.* Long-acting rilpivirine as potential pre-exposure prophylaxis for HIV-1 prevention (the MWRI-01 study): an open-label, Phase I, compartmental, pharmacokinetic and pharmacodynamic assessment. *Lancet HIV* 3(12), e569–e578 (2016).

10. Dou H, Destache CJ, Morehead JR *et al.* Development of a macrophage-based nanoparticle platform for antiretroviral drug delivery. *Blood* 108(8), 2827–2835 (2006).

11. Puligujja P, McMillan J, Kendrick L *et al.* Macrophage folate receptor-targeted antiretroviral therapy facilitates drug entry, retention, antiretroviral activities and biodistribution for reduction of human immunodeficiency virus infections. *Nanomedicine* 9(8), 1263–1273 (2013).

•• **Initial formulation design and development for folic acid decorated antiretroviral drugs for macrophage targeting.**

12. Puligujja P, Balkundi SS, Kendrick LM *et al.* Pharmacodynamics of long-acting folic acid-receptor targeted ritonavir-boosted atazanavir nanoformulations. *Biomaterials* 41, 141–150 (2015).

• **Pharmacodynamics of targeted-nanoformulated antiretroviral therapy.**

13. Dou H, Grotepas CB, Mcmillan JM *et al.* Macrophage delivery of nanoformulated antiretroviral drug to the brain in a murine model of neuroAIDS. *J. Immunol.* 183(1), 661–669 (2009).

14. Arainga M, Guo D, Wiederin J, Ciborowski P, Mcmillan J, Gendelman HE. Opposing regulation of endolysosomal pathways by long-acting nanoformulated antiretroviral therapy and HIV-1 in human macrophages. *Retrovirology* 12, 5 (2015).

• **Introduces the concept that similar subcellular trafficking pathways for nanoparticles and HIV would enhance the antiretroviral response of the drugs.**

15. Gnanadhas DP, Dash PK, Sillman B *et al.* Autophagy facilitates macrophage depots of sustained-release nanoformulated antiretroviral drugs. *J. Clin. Invest.* 127(3), 857–873 (2017).

16. Edagwa B, McMillan J, Sillman B, Gendelman HE. Long-acting slow effective release antiretroviral therapy. *Expert Opin. Drug Deliv.* 14(11), 1281–1291 (2017).

17. Le Douce V, Herbein G, Rohr O, Schwartz C. Molecular mechanisms of HIV-1 persistence in the monocyte-macrophage lineage. *Retrovirology* 7, 32 (2010).

18. Zhu T, Muthui D, Holte S *et al.* Evidence for human immunodeficiency virus type 1 replication *in vivo* in CD14+ monocytes and its potential role as a source of virus in patients on highly active antiretroviral therapy. *J. Virol.* 76(2), 707–716 (2002).

19. Xia W, Hilgenbrink AR, Matteson EL, Lockwood MB, Cheng JX, Low PS. A functional folate receptor is induced during macrophage activation and can be used to target drugs to activated macrophages. *Blood* 113(2), 438–446 (2009).

20. Robertson JD, Rizzello L, Avila-Olias M *et al.* Purification of nanoparticles by size and shape. *Sci. Rep.* 6, 27494 (2016).

21. Gendelman HE, Orenstein JM, Martin MA *et al.* Efficient isolation and propagation of human immunodeficiency virus on recombinant colony-stimulating factor 1-treated monocytes. *J. Exp. Med.* 167(4), 1428–1441 (1988).

22. Zhou T, Su H, Dash P *et al.* Creation of a nanoformulated cabotegravir prodrug with improved antiretroviral profiles. *Biomaterials* 151, 53–65 (2017).

23. Nyaku AN, Kelly SG, Taiwo BO. Long-acting antiretrovirals: where are we now? *Curr. HIV/AIDS Rep.* 14(2), 63–71 (2017).

24. Lembo D, Donalisio M, Civra A, Argenziano M, Cavalli R. Nanomedicine formulations for the delivery of antiviral drugs: a promising solution for the treatment of viral infections. *Expert Opin. Drug Deliv.* 15(1), 93–114 (2018).

25. Owen A, Rannard S. Strengths, weaknesses, opportunities and challenges for long acting injectable therapies: insights for applications in HIV therapy. *Adv. Drug Deliv. Rev.* 103, 144–156 (2016).

26. Remenar JF. Making the leap from daily oral dosing to long-acting injectables: lessons from the antipsychotics. *Mol. Pharm.* 11(6), 1739–1749 (2014).

27. Barnhart M, Shelton JD. ARVs: the next generation. going boldly together to new frontiers of HIV treatment. *Global Health Sci. Pract.* 3(1), 1–11 (2015).

28. Shegokar R, Muller RH. Nanocrystals: industrially feasible multifunctional formulation technology for poorly soluble actives. *Int. J. Pharm.* 399(1–2), 129–139 (2010).

29. Rabinow BE. Nanosuspensions in drug delivery. *Nat. Rev. Drug Discov.* 3(9), 785–796 (2004).

30. Leone F, Cavalli R. Drug nanosuspensions: a ZIP tool between traditional and innovative pharmaceutical formulations. *Expert Opin. Drug Deliv.* 12(10), 1607–1625 (2015).

•• **Comprehensive review on nanocrystal formulation principles, manufacture and applications.**

31. Kumar A, Abbas W, Herbein G. HIV-1 latency in monocytes/macrophages. *Viruses* 6(4), 1837–1860 (2014).

32. Koenig S, Gendelman HE, Orenstein JM *et al.* Detection of AIDS virus in macrophages in brain tissue from aids patients with encephalopathy. *Science* 233(4768), 1089–1093 (1986).
33. Batrakova EV, Gendelman HE, Kabanov AV. Cell-mediated drug delivery. *Expert Opin. Drug Deliv.* 8(4), 415–433 (2011).
34. Kevadiya BD, Woldstad C, Ottemann BM *et al.* Multimodal theranostic nanoformulations permit magnetic resonance bioimaging of antiretroviral drug particle tissue-cell biodistribution. *Theranostics* 8(1), 256–276 (2018).
35. Guo D, Zhou T, Araínga M *et al.* Creation of a long-acting nanoformulated 2′,3′-dideoxy-3′-thiacytidine. *J. Acquir. Immune Defic. Syndr.* 74(3), e75–e83 (2017).
36. Singh D, Mcmillan J, Hilaire J *et al.* Development and characterization of a long-acting nanoformulated abacavir prodrug. *Nanomedicine* 11(15), 1913–1927 (2016).
37. Doshi N, Mitragotri S. Macrophages recognize size and shape of their targets. *PLoS ONE* 5(4), e10051 (2010).
38. Edagwa B, Zhou T, McMillan J, Liu X, Gendelman HE. Development of HIV reservoir targeted long acting nanoformulated antiretroviral therapies. *Curr. Med. Chem.* 21(36), 4186–4198 (2014).
39. Edagwa BJ, Gendelman HE. Antimicrobials: broad-spectrum antivirals. *Nat. Mater.* 17(2), 114–116 (2018).
40. Gunawardana M, Remedios-Chan M, Miller CS *et al.* Pharmacokinetics of long-acting tenofovir alafenamide (GS-7340) subdermal implant for HIV prophylaxis. *Antimicrob. Agents Chemother.* 59(7), 3913–3919 (2015).
41. Agrahari V, Meng J, Ezoulin MJM *et al.* Stimuli-sensitive thiolated hyaluronic acid based nanofibers: synthesis, preclinical safety and *in vitro* anti-HIV activity. *Nanomedicine* 11(22), 2935–2958 (2016).
42. Dutta T, Garg M, Jain NK. Targeting of efavirenz loaded tuftsin conjugated poly(propyleneimine) dendrimers to HIV infected macrophages *in vitro*. *Eur. J. Pharm. Sci.* 34(2–3), 181–189 (2008).
43. Endsley AN, Ho RJY. Enhanced anti-HIV efficacy of Indinavir after inclusion in CD4 targeted lipid nanoparticles. *J. Acquir. Immune Defic. Syndr.* 61(4), 417–424 (2012).
44. Zanotto C, Calderazzo F, Dettin M *et al.* Minimal sequence requirements for synthetic peptides derived from the V3 loop of the human immunodeficiency virus type 1 (HIV-1) to enhance HIV-1 binding to cells and infection. *Virology* 206(2), 807–816 (1995).